"Nano-ion Chromatograph"

Trapping Cations in Specific Positions in Tuneable "Artificial Cell" Channels: New Nanochemistry Perspectives**

Achim Müller, Samar K. Das, Sergei Talismanov, Soumyajit Roy, Eike Beckmann, Hartmut Bögge, Marc Schmidtmann, Alice Merca, Alois Berkle, Lionel Allouche, Yunshan Zhou, and Lijuan Zhang*

Dedicated to Professor Ram Rao on the occasion of his 70th birthday

Molecular dimensioned holes can serve as filters but also trap molecules with well-defined shapes. Whereas a large number of porous materials with cages and tunnels exist as extended structures,[1] as yet not much is known about well-defined, discrete (molecular) nanoporous species. Processes that refer to the entrance of substrates (e.g. of cations) are of particular interest if the affinity of *specific* substrates to *specific* capsule areas can be predicted. This is now possible for nanosized spherical capsules based on the robust fundamental skeleton $(pent)_{12}(linker)_{30} \cong \{(Mo)Mo_5O_{21}(H_2O)_6\}_{12}\{Mo_2O_4(ligand)\}_{30}$[2,3] which has sizeable pores, finely sculpturable interiors and, in between, tuneable functionalized channels with unprecedented molecular-scale filter properties. These will be discussed here for the first time. Most importantly, the channel functionalities as well as the capsule size and charge can be extensively varied, while charge modulations lead to related changes in the affinity to cations! Herein we show that different substrates/cations can be fixed at well-defined positions above, below, and especially in the channels.[3] This situation allows us to study, in principle, new types of molecular transport phenomena, including osmotic-type ones, on the nanoscale, and shows properties of a "nano-ion chromatograph".[4] Additionally, one can construct new geometries such as interpenetrating solids from entering cations owing to the fact that we have a multitude of different as well as equivalent sites in the channels, pores, and in the interior (see also ref. [3b]). This also allows us to study properties of matter under confined conditions.

For the investigations into the uptake of cations and substrates, we used the known capsule **1a**[3] as well as the new

[*] Prof. Dr. A. Müller, Dr. S. K. Das, Dr. S. Talismanov, S. Roy, E. Beckmann, Dr. H. Bögge, M. Schmidtmann, A. Merca, A. Berkle, Dr. L. Allouche, Dr. Y. Zhou, Dr. L. Zhang
Lehrstuhl für Anorganische Chemie I
Fakultät für Chemie der Universität
Postfach 100131, 33501 Bielefeld (Germany)
Fax: (+49) 521-106-6003
E-mail: a.mueller@uni-bielefeld.de

[**] The authors gratefully acknowledge the financial support of the Deutsche Forschungsgemeinschaft, the Fonds der Chemischen Industrie, and the Volkswagen Stiftung. S.R. and A.M. thank the "Graduiertenkolleg Strukturbildungsprozesse", Universität Bielefeld, for their fellowships and L.A. thanks the European Union for a grant (HRPN-CT-1999-0012).

 DOI: 10.1002/ange.200352358

capsule **2a**[5] (both can be easily obtained from **3a**; see Experimental Section) that exhibits the above-mentioned skeleton. As they contain the neutral linker units $\{Mo_2O_4(SO_4)\}$ and $\{Mo_2O_4(HPO_4)\}$, the overall cluster charge corresponds to that of the 12 pentagonal units, that is, $12\times(6-)=72-$.

$(NH_4)_{72-n}[\{(H_2O)_{81-n}+(NH_4)_n\}\subset\{(Mo^{VI})Mo_5^{VI}O_{21}(H_2O)_6\}_{12}$-
$\{Mo_2^{V}O_4(SO_4)\}_{30}]\cdot\approx 200\,H_2O\equiv(NH_4)_{72-n}$-**1a**$\cdot\approx 200\,H_2O$ **1**[2]

$Na_{10}(NH_4)_{62}[\{(Mo^{VI})Mo_5^{VI}O_{21}(H_2O)_6\}_{12}\{Mo_2^{V}O_4(HPO_4)\}_{30}]\cdot$
$\approx[2\,Na^+ + 2\,NH_4^+ + 4\,H_2PO_4^- + 300\,H_2O]$
$\equiv Na_{10}(NH_4)_{62}$-**2a**$\cdot$[crystal ingredients] **2**

$(NH_4)_{42}[\{(Mo^{VI})Mo_5^{VI}O_{21}(H_2O)_6\}_{12}\{Mo_2^{V}O_4(CH_3COO)\}_{30}]\cdot$
$\approx[10\,CH_3COONH_4+300\,H_2O]$
$\equiv(NH_4)_{42}$-**3a**$\cdot$[crystal ingredients] **3**[2b]

The reaction of **1a** and **2a** with different substrates/cations such as Na^+, Cs^+, Ce^{3+}, and $OC(NH_2)NH_3^+$ in aqueous solution leads to the formation of compounds **4**–**7**, respectively, which exhibit well-defined cation separations at, above, or below the capsule's channel-landscapes ("nano-ion chromatography" principle). All compounds were characterized in the solid state by elemental analyses, thermogravimetry (to determine the amount of water of crystallization), single-crystal X-ray diffraction analyses[6] (including bond valence sum (BVS) calculations), IR spectroscopy,[7a] and ^{31}P solid-state NMR[7b] studies.

$Cs_{10}(NH_4)_{52-n}[\{Cs_{10}+(H_2O)_{81-n}+(NH_4)_n\}$
$\subset\{(Mo^{VI})Mo_5^{VI}O_{21}(H_2O)_6\}_{12}\{Mo_2^{V}O_4(SO_4)\}_{30}]\cdot\approx 200\,H_2O$
$\equiv Cs_{10}(NH_4)_{52-n}$-**4a**$\cdot\approx 200\,H_2O$ **4**

$Ce_3(NH_4)_{54}[Ce_3\subset\{(Mo^{VI})Mo_5^{VI}O_{21}(H_2O)_6\}_{12}\{Mo_2^{V}O_4(SO_4)\}_{30}]\cdot$
$\approx 300\,H_2O$
$\equiv Ce_3(NH_4)_{54}$-**5a**$\cdot\approx 300\,H_2O$ **5**

$(NH_3CONH_2)_{28}Na_{11}[\{(NH_3CONH_2)_{20}+Na_{13}\}$
$\subset\{(Mo^{VI})Mo_5^{VI}O_{21}(H_2O)_6\}_{12}\ \{Mo_2^{V}O_4(SO_4)\}_{30}]\cdot\approx 200\,H_2O$
$\equiv(NH_3CONH_2)_{28}Na_{11}$-**6a**$\cdot\approx 200\,H_2O$ **6**

$(NH_4)_{52}[H_{15}\{(Mo^{VI})Mo_5^{VI}O_{21}(H_2O)_6\}_{12}\{Mo_2^{V}O_4(HPO_4)\}_{30}\{Mo^{VI}O_3H\}_5]\cdot$
$\approx[8\,NH_4H_2PO_4+300\,H_2O]$
$\equiv(NH_4)_{52}$-**7a**$\cdot$[crystal ingredients] **7**

$\{(NH_2)_3C\}_{32}[\{(NH_2)_3C)_{20}+(H_2O)_{100}\}\subset\{(Mo^{VI})Mo_5^{VI}O_{21}$-
$(H_2O)_6\}_{12}\{Mo_2^{V}O_4(SO_4)\}_{10}\{Mo_2^{V}O_4(H_2PO_2)\}_{20}]\cdot\approx 100\,H_2O$
$\equiv\{(NH_2)_3C\}_{32}$-**8a**$\cdot\approx 100\,H_2O$ **8**[8]

Whereas the basic skeleton $\{(Mo)Mo_5O_{21}(H_2O)_6\}_{12}\{Mo_2O_4(ligand)\}_{30}$ of the capsule of the precursors **1a** (see refs [2,3]) and **2a** and of the resulting species **4a**–**7a** is the same, **4a**–**7a** show after cation uptake the expected different interiors (Figure 1, 2); this is a situation for molecular materials never observed before. The uptake leads to stoichiometric preferences when the cations are fixed in the higher channel areas, that is, if the $\{Mo_9O_9\}$ pores can function like a type of crown ether. Non-stoichiometric situations can also occur there, but especially below the pore area. In these cases the uptake can be increased by increasing related concentrations and the capsule charge. Whereas the large, stoichiometrically bound, protonated urea cations in **6a** fit reasonably well into the $\{Mo_9O_9\}$ rings/pores (see below), the somewhat smaller Cs^+ ions are not found exactly at the pore centers, but slightly shifted. The even smaller Rb^+ ions show complicated "chameleonic" behavior and are found at several different capsule functionalities, including positions outside the capsule, as there are no characteristic complementary sites available: the Rb^+ ion is too small to be fixed inside the $\{Mo_9O_9\}$ rings and seems to be too large to enter into the channels (see Figure 1). Finally, the much smaller Ce^{3+} ions can enter easily into the capsule interior through the whole channel areas as in **5a**. Comparing the Ce^{3+} behavior with that of Na^+ is especially instructive: Na^+ ions are trapped within the lower part of the channels as they fit exactly into a well-defined site spanned by three oxygen atoms of three SO_4^{2-} ligands (Figure 1 and 2); on the other hand, Ce^{3+} ions are found below the channels and each is coordinated symmetrically in a bidentate fashion to only one SO_4^{2-} ligand. The 30 equivalent Ce^{3+}-type positions span an icosidodecahedron (see below). Importantly, the protonated urea cations in **6a** and also the guanidinium cations in **8a**[8] are noncovalently coordinated to the oxygen atoms of the $\{Mo_9O_9\}$ pores through hydrogen bonds in the usual way known in supramolecular chemistry;[9] a guanidinium cation analogue based on a crown-ether structure has already been described.[9]

The channels of the clusters are lined with nucleo-/hydrophilic chemical groups conducive to the passage of electrophilic (i.e., positively charged) ions:[10] ligands such as sulfate and phosphate promote cation diffusion leading to selectivity and mechanisms controlling the flux. There is also the option of different substrates coordinating simultaneously in the higher and lower parts of the "channels" along the C_3 axes in the direction of the capsule center if the cations are simultaneously present. This offers, in principle, also the possibility to study novel types of cooperativity interactions between different types of encapsulated, fixed cationic centers including paramagnetic ones. When the usual reaction system forming **1a**[2a] is treated with a strong electrolyte solution, such as NaCl in the presence of urea, the cluster anion **1a** "takes up" Na^+ ions before channel "closing" with protonated urea, and forming **6a**. This remarkable preferential trafficking depends specifically on the activity of different functional groups of the capsule.

As the channels' "clothes" can be modified by exchanging ligands attached to the 30 linkers the option exists to use different related functionalities. This is nicely demonstrated by the reaction of **3a** with phosphate ions at different pH values. At about pH 5, the acetate groups are replaced by phosphate groups leading to the formation of **2a**. But if the same reaction is performed at a lower pH (ca. 2; which leads to a partial decomposition of **2a**, that is, with some "molybdate formation"), a novel type of cavity-internal reaction occurs: a nucleation process between the phosphate ligands and the molybdate—released through the preceding reaction—takes place below the $\{Mo_9O_9\}$ rings by linking $\{MoO_3H\}$ groups to phosphate ligands under formation of

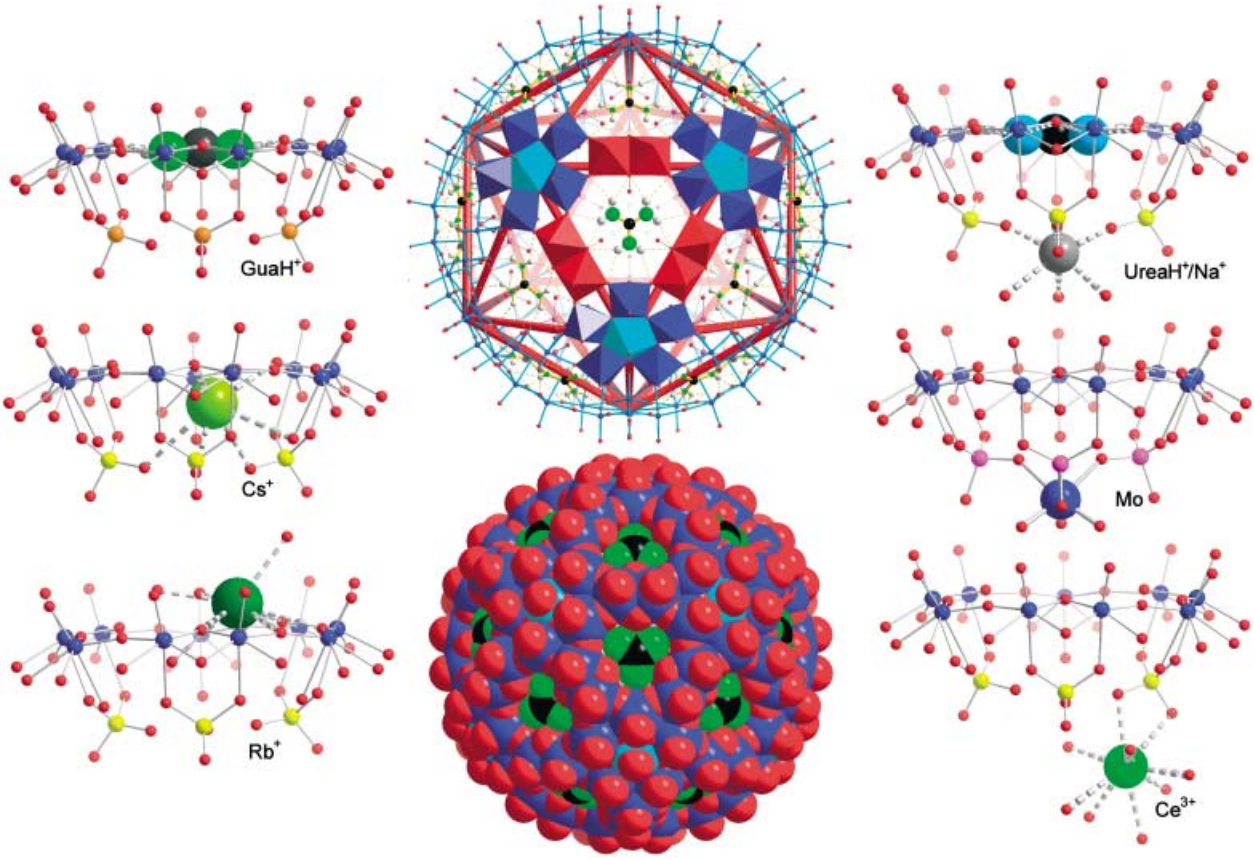

Figure 1. Cations residing at well-defined positions of the capsule of the type $[\{(Mo)Mo_5O_{21}(H_2O)_6\}_{12}\{Mo_2O_4(ligand)\}_{30}]$ with 20 pores and channels. Bottom middle: one whole capsule with guanidinium guests (space-filling); top middle: the main entering portion of one of the 20 $\{Mo_9O_9\}$ pores (with a guanidinium guest) placed on one of the 20 faces of the icosahedron spanned by the 12 central Mo atoms of the pentagonal units in polyhedral representation (see also ref. [3a]). Left and right rows: within the $\{Mo_9O_9\}$ rings/pores the protonated urea (**6a**, top right) and guanidinium cations (**8a**, top left), below, Na^+ within a channel in an environment spanned by three O atoms of three sulfate ligands (**6a**, top right), further below three O atoms of the related phosphate ligands that "fix" the Mo atom of the $\{MoO_3H\}$ group (**7a**, middle right); whereas the rather large Cs^+ ions are found approximately in the pore centers (**4a**, middle left), the small Ce^{3+} ions are positioned below the channels (**5a**, bottom right). As no specific positions are available for Rb^+ ions, these are found in a complicated distribution (only one of which is shown) at several positions even outside the capsule (bottom left). Color code: Mo blue, O red, S yellow, P violet, P/S (of **8**) brown, C black, N green; other respective substrates/cations in different colors.

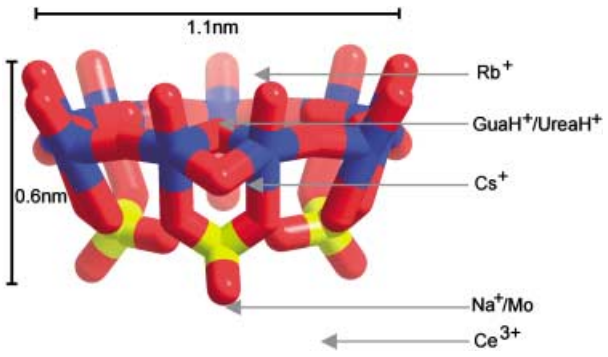

Figure 2. The relative positions of all the fixed substrates in one of the 20 channels (wire-frame representation; color code as in Figure 1).

7a.[11] As geometric constraints allow only for accommodation of up to eight $\{MoO_3H\}$ moieties exactly positioned at the C_3 axes (but according to the underoccupation only five $\{MoO_3H\}$ groups are found), this leads to the generation of a new type of interpenetrating solids in a confined spherical geometry: a cube spanned by eight characteristic $\{MoO_3H\}$-type positions inscribed within a dodecahedron (Figure 3; see also ref. [3b]). The reaction would not occur in case of **1a** with the sulfate channel type, since the relevant anion has a lower electron density at the O atoms and therefore a lower affinity to protonation which is a necessary precondition for a condensation process.

Summary and perspectives: Our capsules can be considered as nanoscale laboratories[12] with a variety of functionalities that enable the positioning of substrates/cations under controlled conditions. Additionally, cation trapping in the 20 pores and channels can be achieved stepwise and several times, respectively, with the consequence that the affinity of the positive substrates to the sites of the negative capsule changes with each cation trapping event due to the decrease of negative charge, a phenomenon which can be regarded as one of the hallmarks of nanotechnology. Interestingly, also capsules with relatively small charges (like that of **3a**) may attract cations, provided that they have a larger charge than the monopositive ones mentioned above: $[M(H_2O)_6]^{2+}$ (M =

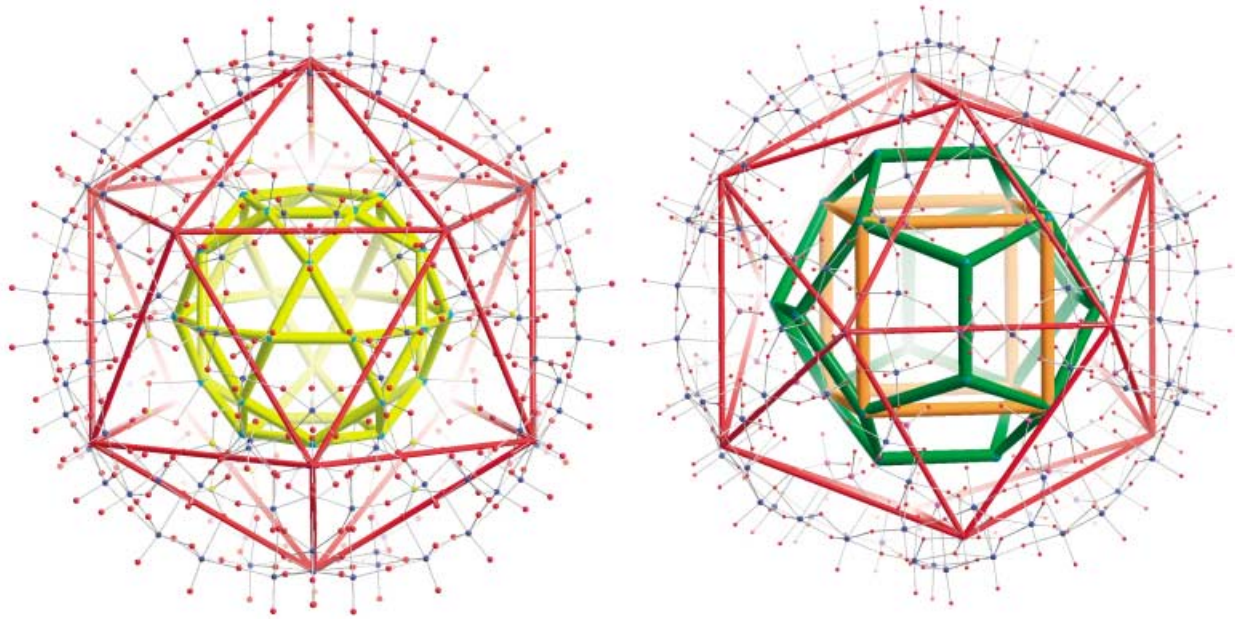

Figure 3. Interpenetrating solids within the capsules of **5a** and **7a** (ball-and-stick model; color code as in Figure 1). Right: a cube (orange) with eight (possible) $\{MoO_3H\}$-type positions as part of the 20 vertices of a dodecahedron (green) spanned by all 20 symmetry-related channel positions on the C_3 axes in **7a** (see also ref. [3b]); left: an icosidodecahedron (yellow) formed by the characteristic Ce^{3+} ion positions of **5a** which are related here to the icosahedron (red) spanned by the 12 central Mo atoms of the pentagonal units—deliberately shown in spite of underoccupation to demonstrate the option of generating different interpenetrating solids.

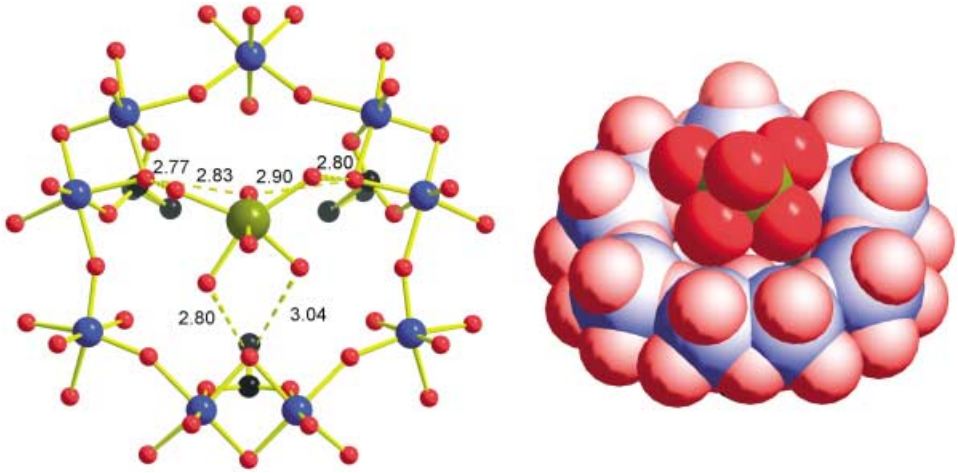

Figure 4. Ball-and-stick (with distances (Å), left) and space-filling representation (right) of one of the $[Ni(H_2O)_6]^{2+}$ complexes interacting through hydrogen bonds with one of the $\{Mo_9O_9\}$ pores of the acetate-type capsule **3a**, leading to the formation of a novel supramolecular cluster arrangement (in the compound about 16 of the 42 NH_4^+ ions of **3a** are replaced by the Ni units; color code as in Figure 1, Ni olive green).

Mg, Ca, Ni) complexes in solution[13] are attracted and fixed through formation of hydrogen bonds between their H_2O ligands and the O atoms in the capsule pores[14] (see Figure 4, which also shows relevant distances). The Ni–O–H···O interactions, that is, second-sphere coordinations, might be considered as an interesting supramolecular cluster phenomenon with perspectives for further investigations.[14] Importantly, the separation of cations in aqueous solution allows, in principle, the option of fabricating a "nano-ion chromatograph", as the "artificial cells" respond to their solute/solvent environment in a specific way. For instance, well-defined, hydrated metal ions such as the above complexes are blocked by the pores because of their size. As the reactions are performed under the conditions of nanocapsule confinement while the capsule size and charge can be precisely generated, new and basic processes may emerge that need not necessarily agree with those observed in bulk materials though also offering new insight into related bulk reactions. For example, it was found very recently that at least five water molecules were necessary to observe dissociation of HBr.[15] Our systems can, generally speaking, provide insight into the influence of geometric confinement on different substrate positionings but especially allow—because of the multitude of different types of equivalent sites—the generation of novel nanoscopic

architectures, for example, with interpenetrating solids like a cube in a dodecahedron (see Figure 3 and refs. [3b, 11]).

Experimental Section

3: Compound **3** was prepared as reported in ref. [5].

2: Compound **3** (3.0 g, 0.11 mmol) was added under constant stirring to a solution of NaH_2PO_4 (3 g, 25 mmol) and NH_4Cl (3 g, 56 mmol) in H_2O (200 mL). The pH was adjusted to ~5 with NH_4OH. The red-brown crystals that precipitated from the solution after five days were filtered off and dried at room temperature. Yield: 1.5 g. Elemental analyses (%) calcd: Na 0.9, N 3.1, P 3.6; found: Na 0.8, N 3.0, P 3.6.

4: A solution of **3** (4.0 g, 0.14 mmol) in H_2O (350 mL) was treated with cesium sulfate (16.5 g, 45.6 mmol) and was stirred at 80 °C for 3 h. The resulting reaction mixture was kept at room temperature for 24 h. The precipitated microcrystalline solid was filtered, washed with water, and dried at room temperature. After the solid was suspended in an ammonium sulfate solution (10.0 g in 350 mL), the suspension was heated at 80 °C for 10–12 min, whereby a clear solution was obtained. The solution was filtered and kept at room temperature for one week in an open 1 L beaker, and red-brown crystals of **4** precipitated. To obtain "better" crystals, the precipitate was redissolved by subsequent warming on a hot plate at 70–80 °C in the same mother liquor by adding water (130 mL), and the resulting clear solution was kept in the same open beaker for one week. The precipitated brown rhombohedral crystals, which are more suitable for a structure determination than the first precipitated crystals crystallizing in the cubic space group showing a problematical disorder, were filtered, washed with 2-propanol, and dried at room temperature. Yield: 2.1 g. Elemental analyses (%) calcd: Cs 8.7, N 2.4, S 3.1; found: Cs 8.7, N 2.5, S 3.4.

5: $CeCl_3 \cdot 7H_2O$ (10.0 g, 26.8 mmol) was added after 1.5 h to a refluxing solution of **3** (5.0 g, 0.18 mmol) and ammonium sulfate (15.0 g, 113.5 mmol) in H_2O (400 mL). The resulting solution was refluxed for 30 min and filtered hot. The dark brown crystals of **4** that precipitated after one day were filtered, washed with ice-cold 2-propanol, and dried in air. Yield: 4.4 g. Elemental analyses (%) calcd: Ce 2.9, N 2.6, S 3.2; found: Ce 2.6, N 3.0, S 3.6.

6: A mixture of **3** (0.5 g, 0.02 mmol), urea (1.0 g, 16.7 mmol), $(NH_4)_2SO_4$ (2.5 g, 18.9 mmol), H_2O (40 mL), and 16% HCl (8 mL) in a 100-mL Erlenmeyer flask (covered with a watch-glass) was heated to 60–70 °C. After 90 min, NaCl (3.0 g, 51.3 mmol) was added and the solution was heated for 90 min and then kept at room temperature. After 3–4 days brown rhombohedral crystals of **6** were filtered off, washed with a small amount of ice-cold water, then with ice-cold 2-propanol, and dried in air. Yield: 0.35 g. Elemental analyses (%) calcd: Na 1.9, C 1.9, N 4.6; found: Na 2.1, C 1.8, N 4.6.

7: Compound **3** (3.0 g, 0.11 mmol) was added under constant stirring (15 min) to a solution of $NH_4H_2PO_4$ (3 g, 26 mmol), NH_4Cl (3 g, 56 mmol) and HCl (15 mL, 1M) in H_2O (200 mL). After the solution was kept in an open beaker at room temperature for seven days, the precipitated red-brown crystals of **7** were filtered off and dried at room temperature. Yield: 2.0 g. Elemental analyses (%) calcd: N 2.8, P 3.9; found: N 2.8, P 3.9.

The chemical formulas refer to the maximum number of water molecules in the crystal, which is in agreement with the cell volume. According to the observed loss of water the analytical data, however, refer to this number of crystal water molecules minus 50.

Received: July 11, 2003 [Z52358]
Published Online: October 8, 2003

Keywords: confined geometries · encapsulation · ion transport/uptake · nanotechnology · porous materials

[1] a) *Handbook of Porous Solids* (Eds.: F. Schüth, K. S. W. Sing, J. Weitkamp), Wiley-VCH, Weinheim, **2002**; b) M. A. White, *Properties of Materials*, Oxford University Press, New York, **1999**, chap.: Inclusion Compounds; c) G. Férey, *Science* **2001**, *291*, 994–995.

[2] a) A. Müller, E. Krickemeyer, H. Bögge, M. Schmidtmann, B. Botar, M. O. Talismanova, *Angew. Chem.* **2003**, *115*, 2131–2136; *Angew. Chem. Int. Ed.* **2003**, *42*, 2085–2090; b) A. Müller, E. Krickemeyer, H. Bögge, M. Schmidtmann, F. Peters, *Angew. Chem.* **1998**, *110*, 3567–3571; *Angew. Chem. Int. Ed.* **1998**, *37*, 3360–3363.

[3] a) A. Müller, P. Kögerler, C. Kuhlmann, *Chem. Commun.* **1999**, 1347–1358; b) A. Müller, *Science* **2003**, *300*, 749–750. c) The term stability refers here to the fact that at least in the final product always the same type of well-defined capsules are found with the expected functionalities after reactions have taken place in solution. But, in principle, it cannot be excluded that in solution the pores, that is, the $\{Mo_9O_9\}$ rings, are opened slightly during uptake. Related solution NMR studies concerning the stability and reaction pathways are currently possible and are in progress (F. Taulelle, M. Henry, A. Müller; see also ref. [5]).[16]

[4] See also related discussion in: M. Gross, *Chem. Br.* **2003**, *39* (August Issue), p. 18. As the cations entering through the gates are not randomly distributed in the cell interior but fixed at functionalities according to their specific properties, thus relatively reducing the whole capsule system entropy, a situation results that is formally comparable to that of "Maxwell's Demon", but acting in a closed system (the related Gedanken experiment is for instance explained in textbooks of Statistical Thermodynamics and even in *The New Encyclopaedia Britannica, Vol. 23*, 15th ed., Encyclopaedia Britannica, Chicago, **2002**, p. 692, including the statement: "The hypothetical intelligent being known as Maxwell's demon was a factor in the development of information theory"). See also: M. Gross, *Travels to the Nanoworld: Miniature Machinery in Nature and Technology*, Perseus Publishing, Cambridge, Massachusetts, **2001** (Chapter: Maxwell's demon—a predecessor of nanotechnology?); D. E. H. Jones, *Nature* **1995**, *374*, 835–837.

[5] Both are formed by ligand exchange from **3a**, which is available in facile syntheses according to: L. Cronin, E. Diemann, A. Müller in *Inorganic Experiments* (Ed.: J. D. Woollins), 2nd ed., Wiley-VCH, Weinheim, **2003**, pp. 340–346 and A. Müller, S. K. Das, E. Krickemeyer, C. Kuhlmann, *Inorg. Synth.* **2003**, *34*, in press. The sulfate cluster anion **1a**[2a] with the high charge of 72− is formed from **3a** in situ in solution during the processes leading to **4a, 5a**, and **6a**, which can also be obtained by starting from solutions of crystalline **1**. Important in context with footnote [3] is that **1a** can be obtained by ligand exchange from **3a** without heating, that is at room temperature and under low pH conditions which supports the release of the leaving group acetic acid.

[6] Crystal data for **2**: $H_{1038}Mo_{132}N_{64}Na_{12}O_{880}P_{34}$, $M_r = 30015.89\ g\,mol^{-1}$, cubic space group $Fm\bar{3}$, $a = 45.6162(12)$ Å, $V = 94920(4)$ Å^3, $Z = 4$, $\rho = 2.100\ g\,cm^{-3}$, $\mu = 1.862\ mm^{-1}$, $F(000) = 58848$, crystal size $= 0.24 \times 0.24 \times 0.24\ mm^3$. A total of 120764 reflections ($0.77 < \Theta < 25.02°$) were collected, of which 7311 reflections were unique ($R(int) = 0.0578$). $R = 0.0832$ for 4974 reflections with $I > 2\sigma(I)$, $R = 0.1464$ for all reflections, max./min. residual electron density 1.316 and $-1.715\ e\,Å^{-3}$. Crystal data for **4**: $H_{914}Cs_{20}Mo_{132}N_{52}O_{845}S_{30}$, $M_r = 31453.91\ g\,mol^{-1}$, rhombohedral space group $R\bar{3}$, $a = 32.7258(8)$, $c = 73.664(3)$ Å, $V = 68323(3)$ Å^3, $Z = 3$, $\rho = 2.293\ g\,cm^{-3}$, $\mu = 2.725\ mm^{-1}$, $F(000) = 45486$, crystal size $= 0.25 \times 0.20 \times 0.15\ mm^3$. A total of 188827 reflections ($0.77 < \Theta < 30.01°$) were collected, of which 44291 reflections were unique ($R(int) = 0.0564$). $R = 0.0498$ for 32184 reflections with

$I > 2\sigma(I)$, $R = 0.0789$ for all reflections, max./min. residual electron density 2.369 and $-1.403\ e\,Å^{-3}$. Crystal data for **5**: $H_{960}Ce_6Mo_{132}N_{54}O_{864}S_{30}$, $M_r = 30014.82\ g\,mol^{-1}$, rhombohedral space group $R\bar{3}$, $a = 32.7411(7)$, $c = 73.682(2)$ Å, $V = 68404(3)$ Å^3, $Z = 3$, $\rho = 2.186\ g\,cm^{-3}$, $\mu = 2.229\ mm^{-1}$, $F(000) = 43866$, crystal size $= 0.40 \times 0.25 \times 0.20\ mm^3$. A total of 136090 reflections ($0.77 < \Theta < 27.02°$) were collected, of which 33123 reflections were unique ($R(\text{int}) = 0.0277$). $R = 0.0424$ for 27495 reflections with $I > 2\sigma(I)$, $R = 0.0559$ for all reflections, max./min. residual electron density 2.242 and $-1.215\ e\,Å^{-3}$. Crystal data for **6**: $C_{48}H_{784}Mo_{132}N_{96}Na_{24}O_{812}S_{30}$, $M_r = 29881.35\ g\,mol^{-1}$, rhombohedral space group $R\bar{3}$, $a = 32.8028(5)$, $c = 73.948(2)$ Å, $V = 68910(2)$ Å^3, $Z = 3$, $\rho = 2.160\ g\,cm^{-3}$, $\mu = 1.933\ mm^{-1}$, $F(000) = 43584$, crystal size $= 0.25 \times 0.25 \times 0.15\ mm^3$. A total of 190772 reflections ($0.77 < \Theta < 30.02°$) were collected, of which 44749 reflections were unique ($R(\text{int}) = 0.0358$). $R = 0.0395$ for 36437 reflections with $I > 2\sigma(I)$, $R = 0.0556$ for all reflections, max./min. residual electron density 2.527 and $-1.426\ e\,Å^{-3}$. Crystal data for **7**: $H_{1050}Mo_{137}N_{60}O_{911}P_{38}$, $M_r = 30795.64\ g\,mol^{-1}$, cubic space group $Fm\bar{3}$, $a = 45.6587(12)$ Å, $V = 95186(4)$ Å^3, $Z = 4$, $\rho = 2.149\ g\,cm^{-3}$, $\mu = 1.925\ mm^{-1}$, $F(000) = 60328$, crystal size $= 0.24 \times 0.24 \times 0.24\ mm^3$. A total of 118119 reflections ($0.77 < \Theta < 25.03°$) were collected, of which 7327 reflections were unique ($R(\text{int}) = 0.0643$). $R = 0.0883$ for 5296 reflections with $I > 2\sigma(I)$, $R = 0.1371$ for all reflections, max./min. residual electron density 1.701 and $-1.782\ e\,Å^{-3}$. Crystals of **2, 4, 5, 6**, and **7** were removed from the mother liquor and immediately cooled to 173–193 K on a Bruker AXS SMART diffractometer (three-circle goniometer with 1 K CCD detector, $Mo_{K\alpha}$ radiation, graphite monochromator; hemisphere data collection in ω at 0.3° scan width in three runs with 606, 435, and 230 frames ($\phi =$ 0, 88, and 180°) at a detector distance of 4.0–5.0 cm). For all structures empirical absorption corrections were performed by using equivalent reflections with the program SADABS 2.03. The structures were solved with the program SHELXS-97 and refined by using SHELXL-93. (SHELXS/L, SADABS from G. M. Sheldrick, University of Göttingen (Germany) **1993/97**; structure graphics with DIAMOND 2.1 from K. Brandenburg, Crystal Impact GbR, **2001**). Further details of the crstal structure investigations can be obtained from the Fachinformationszentrum Karlsruhe, 76344 Eggenstein-Leopoldshafen, Germany, (fax: (+49)7247-808-666; e-mail: crysdata@fiz.karlsruhe.de) on quoting the depository numbers CSD-413251 (**2**), CSD 413252 (**4**), CSD 413253 (**5**), CSD 413254 (**6**) and CSD 413255 (**7**).

[7] a) Characteristic IR bands (solid, KBr pellet, $\tilde{\nu}$) for compounds **1–8** due to presence of the [{(Mo)Mo_5}$_{12}${Mo_2}$_{30}$]-type skeleton (variations $\pm 3\ cm^{-1}$): 970s, [ν(Mo=O)], 860m, 800vs, 725vs, 570s; **2** shows additionally bands at 1107, 1050, 1009 [ν(P–O)] and **4, 5, 6** at 1140 (m), 1035 cm^{-1} (w–m, $\nu_{as}(SO_4)$); **6** shows weak urea bands and **2, 4, 5, 7** the $\delta(NH_4)$ bands at $\approx 1400\ cm^{-1}$. b) ^{31}P MAS NMR spectra allow us to distinguish between the "phosphates" coordinated as ligands and those abundant in the crystal lattice.

[8] A. Müller, E. Krickemeyer, H. Bögge, M. Schmidtmann, S. Roy, A. Berkle, *Angew. Chem.* **2002**, *114*, 3756–3761; *Angew. Chem. Int. Ed.* **2002**, *41*, 3604–3609.

[9] J.-M. Lehn, *Supramolecular Chemistry: Concepts and Perspectives*, VCH, Weinheim, **1995**, p. 28.

[10] For the transport of the cations through biological membranes, negatively charged amino acids play a key role; see: D. Voet, J. G. Voet, *Biochemistry*, 2nd ed., Wiley, New York, **1995**, chap. 18.

[11] The situation is comparable to the formation of P-O-Mo bonds during the synthesis of the $[PMo_{12}O_{40}]^{3-}$ Keggin anion at low pH values. In **7a** the phosphate ligands, instead of being positioned exactly below the {Mo_2} groups, "are oriented" slightly towards the {MoO_3H} group. Consequently, a {MoO_3H} moiety is not found in all 20 channels/sites, hence not a dodecahedron is generated by 20 {MoO_3H} groups but "only" a cube with eight of these can be formed. (This can be visualized as only two of each of the dodecahedral pentagon vertices can be involved as sites for {MoO_3H}. As three pentagonal faces are connected at each vertex this leads to a total number of $8 = (12 \times 2)/3$ positions; see Figure 3).

[12] For related topics see: a) K. E. Drexler, *Nanosystems: Molecular Machinery, Manufacturing, and Computation*, Wiley, New York, **1992**; b) *Recent Advances in the Chemistry of Nanomaterials* (Eds.: C. N. R. Rao, A. Müller, A. K. Cheetham), Wiley-VCH, Weinheim, in press; c) P. Ball, *Made to Measure*: *New Materials for the 21st Century*, Princeton University Press, Princeton, **1997**; regarding the importance of pores see also: d) J. Tersoff, *Nature* **2001**, *412*, 135–136.

[13] D. T. Richens, *The Chemistry of Aqua Ions*, Wiley, Chichester, **1997** (Ni^{2+} has a well-defined, rather strongly bonded primary hydration sphere in aqueous solution, for example, compared to Ce^{3+}).

[14] The phenomenon of trapping aqueous solutes/complexes will be studied separately: A. Müller, Y. Zhou, L. Zhang, L. Toma, H. Bögge, M. Schmidtmann, unpublished results.

[15] A. F. Voegele, K. R. Liedl, *Angew. Chem.* **2003**, *115*, 2162–2164; *Angew. Chem. Int. Ed.* **2003**, *42*, 2114–2116.

[16] **Note added in proof** (Setember 24, 2003): According to new NMR investigations (F. Taulelle, M. Henry, A. Müller) the stability of the capsule in solution is very high. Furthermore the exchange of the acetate ligands of the starting material **3a** is easily possible under low pH conditions (see also ref. [5]).

